# Physical and Chemical Characteristics Affecting the Durability of Concrete

Vagelis Papadakis, Costas Vayenas, Michael Fardis

# Physical and Chemical Characteristics Affecting the Durability of Concrete

by Vagelis G. Papadakis, Costas G. Vayenas, and Michael N. Fardis

*The durability of reinforced concrete is influenced by those physical characteristics of concrete that control the dif of gases, such as $CO_2$ and $O_2$, or of liquids (mainly water) through its pores, and the diffusion of ions, such as $Cl^-$, dissolved in the pore water. These physical characteristics depend on the composition of concrete, the chemical composition and type of cement, and the relative humidity and temperature of the environment. In the present paper, these characteristics of concrete are determined analytically and/or experimentally in terms of the composition parameters and environmental conditions: the molar concentration of those constituents that are susceptible to carbonation; the porosity and pore-size distribution; the degree of saturation of the pores; and the effective dif of gases through the concrete.*

**Keywords:** concrete **durability**; diffusion; diffusivity; hydration; **porosity**; pozzolans; **reinforced concretes**; saturation; specific surface.

The good performance of concrete in service, including its durability, is a major factor for its success as a construction material. This is particularly true of its application, in the form of reinforced concrete, as a structural material, since its major competitors, steel and timber, have inherent durability limitations. However, the last two decades have seen a disconcerting increase in examples of the unsatisfactory durability of concrete structures, especially reinforced concrete ones. Since the state of the art of concrete and reinforced concrete durability has enjoyed a relatively short research history compared to strength, durability has replaced strength as the number one issue concerning the engineering community today.

Deterioration of concrete in service may be the result of a variety of physical and chemical processes,[1,2] such as attack by acids, sulfates, or alkalis, alkali-aggregate reactions, freeze-thaw cycles, etc. In reinforced concrete, the most serious deterioration mechanisms are those leading to corrosion of the reinforcement, resulting in a reduction in the effective cross-sectional area of reinforcing bars, and in ultimate disruption of the concrete due to spalling of the concrete cover. Reinforcement corrosion occurs only after depassivation due to carbonation of the surrounding concrete, penetration of chloride ions, or a combination of both.[1,2] All processes causing deterioration of the concrete itself or corrosion of the reinforcement involve transport phenomena through the pores of the concrete. These transport mechanisms include diffusion of such gases as $O_2$, $CO_2$, or $SO_2$ in the gaseous phase of the pores, from the environment to interior regions where the gas concentration is low due to gas consumption (by carbonation for $CO_2$ and corrosion of the steel for $O_2$). They also include diffusion of aggressive ions dissolved in the pore water, again from the external surfaces to interior regions of consumption and low concentration. These dissolved aggressive ions can be $Cl^-$, $H^+$, or $SO_4^{2-}$, originating from dissociation of dissolved acids, alkali ions, $Na^+$, etc. Flow of water through the pores is also possible due to capillary suction or hydraulic pressure gradients. Finally, it is in the pore water that most of the chemical reactions between the externally supplied aggressive substances and the constituents of cement and concrete take place. Therefore, to study, describe quantitatively, and ultimately limit or control these transport phenomena and the deterioration of concrete, knowledge of the structure of its pores and distribution of the pore volume into gaseous and aqueous phases is absolutely necessary. In addition, one needs to know the evolution in time of the concentrations of those constituents of cement, hydrated or not, that are expected to react with the externally supplied aggressive substances.

Significant work on hydration reactions and mechanisms has already been done by previous workers.[3-7] The literature is also rich in concrete porosity and pore-

*Vagelis G. Papadakis is a graduate student in the Department of Chemical Engineering of the University of Patras, Greece, and in the Institute of Chemical Engineering and High Temperature Chemical Processes. He holds a Diploma in Chemical Engineering from the University of Patras and is working toward a PhD in the area of carbonation and durability of concrete.*

*Costas G. Vayenas is a Professor of Reaction Engineering and Catalysis in the Chemical Engineering Department of the University of Patras and a researcher in the Institute of Chemical Engineering and High Temperature Chemical Processes. He holds a PhD in Chemical Engineering from the University of Rochester. Prior to joining the faculty at the University of Patras, he was Assistant Professor at Yale and Associate Professor at M.I.T. He has authored many papers on catalysis, high-temperature Electrochemistry, and mathematical modeling of chemical processes.*

*ACI member Michael N. Fardis is a Professor of Concrete Structures in the Civil Engineering Department of the University of Patras. He holds an M.Sc. and PhD in Civil Engineering from M.I.T. Prior to joining the faculty at the University of Patras, he was an Associate Professor at M.I.T. He has authored many papers, mainly on analytical and numerical modeling of concrete and concrete structures.*

size distribution measurements,[8-20] studies of water behavior in hardened cement,[2,4,8,21,22] and measurements of gas diffusion through the concrete pores.[17,23-25] What is lacking, though, are quantitative predictive models for these physical and chemical characteristics, in terms of the composition parameters and environmental conditions.

## RESEARCH SIGNIFICANCE

Quantitative prediction and control of the evolution in time of physicochemical processes preceding corrosion of reinforcing bars, such as the reduction in alkalinity due to carbonation of concrete or the diffusion of $Cl^-$ in the pore water, and processes that take place simultaneously with corrosion, such as diffusion of $O_2$ through the pores, require knowledge of some physical characteristics of concrete, such as porosity, pore-size distribution, degree of saturation of the pores, and gas diffusivity, as well as the amount of carbonatable materials in concrete, etc. Computed and measured values of these characteristics or parameters are presented in this paper for portland cement in terms of the composition parameters of concrete, chemical composition of cement, and environmental parameters, such as ambient relative humidity. In a separate paper, the effect of pozzolans on these characteristics or parameters will be discussed.

## MOLAR CONCENTRATION OF CARBONATABLE CONSTITUENTS OF HARDENED CEMENT PASTE

The major constituents of hardened cement paste subject to carbonation in the presence of moisture are $Ca(OH)_2$ and calcium silicate hydrate (CSH). Prior to their hydration, calcium silicates $C_3S$ and $C_2S$ are also subject to carbonation. For the other hydrated or unhydrated constituents of hardened cement paste, carbonation seems to be limited to a surface zone, without affecting the bulk of the crystallites.[5] Therefore, it is the molar concentrations of $Ca(OH)_2$, CSH, and the yet unhydrated amounts of $C_3S$ and $C_2S$ that are of interest as far as carbonation is concerned. These constituents of cement are produced or consumed by the chemical reactions of hydration. Using the notation of cement technology,* the hydration reactions of ordinary portland cement (OPC) in the presence of gypsum are[3-7]

$$2C_3S + 6H \xrightarrow{r_{H,C_3S}} C_3S_2H_3 + 3CH \quad (1)$$

$$2C_2S + 4H \xrightarrow{r_{H,C_2S}} C_3S_2H_3 + CH \quad (2)$$

$$C_4AF + 2CH + 2C\bar{S}H_2 + 18H \xrightarrow{r_{H,C_4AF}} C_8AF\bar{S}_2H_{24} \quad (3)$$

$$C_3A + C\bar{S}H_2 + 10H \xrightarrow{r_{H,C_3A}} C_4A\bar{S}H_{12} \quad (4)$$

$$C_4AF + 4CH + 22H \xrightarrow{r_{H,C_4AF}} C_8AFH_{26} \quad (5)$$

$$C_3A + CH + 12H \xrightarrow{r_{H,C_3A}} C_4AH_{13} \quad (6)$$

The previous hydration reactions take place at molar rates per unit concrete volume $r_{H,i}$ ($i$ = $C_3S$, $C_2S$, $C_4AF$, $C_3A$) in mol/m³ · sec. The presence of gypsum has only a minor effect on the rates of hydration of $C_3A$ and $C_4AF$, so that Reactions (3) and (4) can be taken to have the same rate as Reactions (5) and (6), respectively,[6] i.e., $r_{H,C_4AF}$ and $r_{H,C_3A}$. Expressions for the rates $r_{H,i}$ can be obtained from measurements of the fraction $F_i(t)$ of compound $i$, which has been hydrated at time $t$ (in sec) after mixing. Such measurements have been presented in the past by Brunauer and Copeland[3] and more recently by Taylor,[7] and point to expression of the form

$$r_{H,i} \equiv -d[i]/dt = k_{H,i}\,[i]^{n_i}/[i]_0^{n_i-1} \quad (7)$$

$$F_i(t) = 1 - [i]/[i]_0 = 1 - (1 - k_{H,i}\,t(1-n_i))^{1/(1-n_i)} \quad (8)$$

in which $[i]$ and $[i]_0$ are the current and initial (at $t$ = 0) molar concentrations of compound $i$, respectively (in mol/m³). Fitted values of the exponents $n_i$ and the coefficients $k_{H,i}$ are listed in Table 1, and the resulting $F_i(t)$-curves are compared in Fig. 1 to measured values. Table 1 and Fig. 1 can be considered to apply to OPC of normal fineness, corresponding to Type I cement.

In the presence of gypsum, Reactions (3) and (4) dominate over Reactions (5) and (6),[5,6] so Reactions (5) and (6) take place only after all the gypsum has been consumed. This happens at a time $t^*$, which can be determined from the condition

$$[C_3A]_0 F_{C_3A}(t^*) + 2\,[C_4AF]_0\,F_{C_4AF}(t^*) = [C\bar{S}H_2]_0 \quad (9a)$$

*Cement technology notation: C:CaO, S:$SiO_2$, A:$Al_2O_3$, F:$Fe_2O_3$, H:$H_2O$, $\bar{S}$:$SO_3$, $\bar{C}$:$CO_2$, and therefore: $C_3S$:3CaO•2$SiO_2$, CH:Ca(OH)$_2$, $C_3S_2H_3$ (or CSH): 3CaO•2$SiO_2$•3$H_2O$, $C\bar{S}H_2$: $CaSO_4$•2$H_2O$, etc.

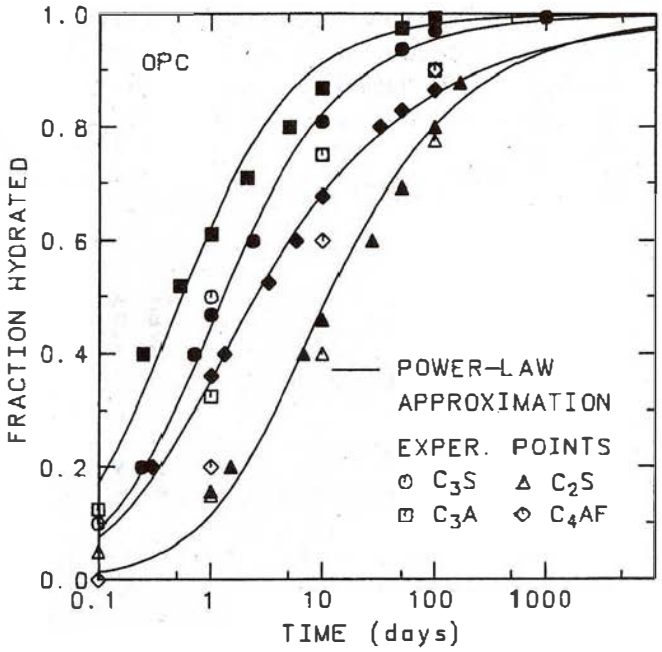


*Fig. 1—Speed of hydration of the four major constituents of OPC, filled points by Brunauer and Copeland[3]; open points by Taylor[7]*

**Table 1—Parameters of major constituents of ordinary portland cement**

| Compound | $C_3S$ | $C_2S$ | $C_4AF$ | $C_3A$ | $C\bar{S}H_2$ |
|---|---|---|---|---|---|
| Exponent $n_i$, Eq. (8) | 2.65 | 3.10 | 3.81 | 2.41 | — |
| Coefficient $k_{H,i}$ (20 C) x $10^5$ ($s^{-1}$), Eq. (8) | 1.17 | 0.16 | 1.00 | 2.46 | — |
| Molar weight $MW_i$ x $10^3$, kg/mol | 228.30 | 172.22 | 485.96 | 270.18 | 172.17 |
| Molar volumes differences | | | | | |
| Hydration reaction | (1) | (2) | (3) | (4) | (5) | (6) |
| $\Delta\bar{V}$ x $10^6$, $m^3$/mol | 53.28 | 39.35 | −220 | 155.86 | −230 | 149.82 |

The value of $t^*$ can be found numerically, from an exponential in $t^*$ equation, which results from substitution of $F_{C_3A}(t^*)$ and $F_{C_4AF}(t^*)$ from Eq. (8) in terms of $t^*$. The second term in Eq. (9a) can be considered negligible, because $SO_4^{2-}$ ions react preferentially with $C_3A$ rather than with $C_4AF$,[6] so the value of $t^*$ can be computed in approximation

$$t^* = \frac{1}{k_{H,C_3A}(1 - n_{C_3A})} \left[1 - \left(1 - \frac{[C\bar{S}H_2]_0}{[C_3A]_0}\right)^{(1-n_{C_3A})}\right] \quad (9b)$$

The molar concentrations of the carbonatable constituents at time $t$ after mixing are, therefore, equal to

$$[Ca(OH)_2] = \frac{3}{2}[C_3S]_0F_{C_3S} + \frac{1}{2}[C_2S]_0F_{C_2S} - 2[C_4AF]_0F_{C_4AF},\ 0 \leq t \leq t^* \quad (10a)$$

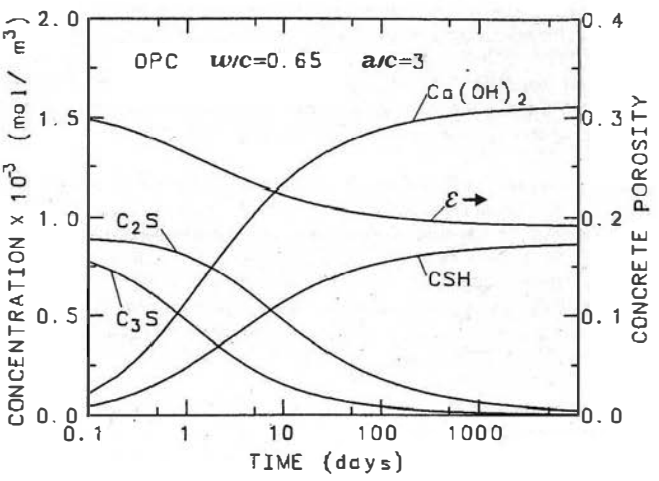


*Fig. 2—Evolution with age of the molar concentration of the carbonatable constituents and porosity of OPC*

$$[Ca(OH)_2] = \frac{3}{2}[C_3S]_0F_{C_3S} + \frac{1}{2}[C_2S]_0F_{C_2S} - 4[C_4AF]_0F_{C_4AF} - [C_3A]_0F_{C_3A} + [C\bar{S}H_2]_0,\ t \geq t^* \quad (10b)$$

$$[CSH] = \frac{1}{2}[C_3S]_0F_{C_3S} + \frac{1}{2}[C_2S]_0F_{C_2S} \quad (11)$$

$$[C_3S] = [C_3S]_0(1 - F_{C_3S}) \quad (12)$$

$$[C_2S] = [C_2S]_0(1 - F_{C_2S}) \quad (13)$$

The initial molar concentrations of compound $i$ ($i$ = $C_3S$, $C_2S$, $C_4AF$, $C_3A$) and of gypsum, denoted by $[i]_0$ and $[C\bar{S}H_2]_0$, respectively, in OPC concrete can be computed from: a) the weight fraction of clinker and gypsum in OPC, denoted by $m_{cl}$ and $m_{gy} = 1 - m_{cl}$, respectively; b) the weight fraction of compound $i$ in the clinker $m_i$ which can be calculated from oxide analysis;[4] c) the mix proportions of concrete, i.e., the water-cement ratio $w/c$, the aggregate-cement ratio $a/c$, and the volume fraction of concrete in entrapped or entrained air $\epsilon_{air}$

$$[i]_0 = \frac{m_i m_{cl} \rho_c (1 - \epsilon_{air})}{MW_i\left(1 + \frac{w}{c}\frac{\rho_c}{\rho_w} + \frac{a}{c}\frac{\rho_c}{\rho_a}\right)} \quad (14)$$

$$[C\bar{S}H_2]_0 = \frac{m_{gy} \rho_c (1 - \epsilon_{air})}{MW_{gy}\left(1 + \frac{w}{c}\frac{\rho_c}{\rho_w} + \frac{a}{c}\frac{\rho_c}{\rho_a}\right)} \quad (15)$$

in which $\rho_c$, $\rho_w$, and $\rho_a$ (in kg/m³) are the densities of cement, water, and aggregates, respectively, and $MW_i$, $MW_{gy}$ are the molar weights of compound $i$ and $C\bar{S}H_2$, respectively, given in Table 1 in kg/mol.

Fig. 2 shows the evolution in time of the molar concentrations of the carbonatable constituents of con-

crete, according to Eq. (10) through (13) for ordinary portland cement, and for $w/c = 0.65$ and $a/c = 3$. Fig. 3 presents the final concentrations of $Ca(OH)_2$ and CSH for various mix proportions of concrete and for fully hydrated OPC.

## POROSITY OF CONCRETE

The porosity of concrete $\epsilon$, defined as the ratio of pore volume to the total volume of concrete, decreases with time due to the processes of cement hydration and of carbonation

$$\epsilon(t) = \epsilon_0 - \Delta\epsilon_H(t) - \Delta\epsilon_c \qquad (16)$$

in which $\epsilon_0$ is the porosity of fresh concrete and $\Delta\epsilon_H(t)$, $\Delta\epsilon_c$ correspond to the reduction in porosity due to hydration and carbonation, respectively. The initial value of porosity $\epsilon_0$ is the sum of the volume fractions of mixing water and entrapped (or entrained plus entrapped, in air-entrained concrete) air. The volume fraction of entrapped (or entrained) air, denoted by $\epsilon_{air}$, is in the range of a few percent, depending on the maximum aggregate size,[26] whereas the volume fraction of water in fresh concrete equals the mass of water per unit volume of concrete divided by the mass density of water. In terms of the composition parameters of concrete, i.e., of the water-cement ratio $w/c$, and the aggregate-cement ratio $a/c$, the initial porosity equals

$$\epsilon_0 = \frac{\frac{w}{c}\frac{\rho_c}{\rho_w}(1 - \epsilon_{air})}{\left(1 + \frac{w}{c}\frac{\rho_c}{\rho_w} + \frac{a}{c}\frac{\rho_c}{\rho_a}\right)} + \epsilon_{air} \qquad (17)$$

The reduction in porosity due to hydration $\Delta\epsilon_H(t)$ is due to the fact that the molar volume of the solid products of hydration, in the right-hand side of Eq. (1) through (6), exceeds that of the solid reactants, in the left-hand side of these equations. So, if $\Delta\bar{V}_{C_3S}$, $\Delta\bar{V}_{C_2S}$, $\Delta\bar{V}_{C_4AF,S}$, $\Delta\bar{V}_{C_3A,S}$, $\Delta\bar{V}_{C_4AF}$, and $\Delta\bar{V}_{C_3A}$ are the differences in molar volumes between solid reaction products and solid reactants in the hydration reactions, Eq. (1) through (6), respectively (given in Table 1, in $m^3$ per reacting mole of compound $i$), then

$$\Delta\epsilon_H(t) = [C_3S]_0 F_{C_3S}\Delta\bar{V}_{C_3S} + [C_2S]_0 F_{C_2S}\Delta\bar{V}_{C_2S} + [C_3A]_0 F_{C_3A}\Delta\bar{V}_{C_3A,\bar{S}} + [C_4AF]_0 F_{C_4AF}\Delta\bar{V}_{C_4AF,\bar{S}},\ 0 \leq t \leq t^* \qquad (18a)$$

$$\Delta\epsilon_H(t) = [C_3S]_0 F_{C_3S}\Delta\bar{V}_{C_3S} + [C_2S]_0 F_{C_2S}\Delta\bar{V}_{C_2S} + [C_3A]_0 F_{C_3A}(t^*)\Delta\bar{V}_{C_3A,\bar{S}} + [C_3A]_0 (F_{C_3A} - F_{C_3A}(t^*))\Delta\bar{V}_{C_3A} + [C_4AF]_0 F_{C_4AF}(t^*)\Delta\bar{V}_{C_4AF,\bar{S}} + [C_4AF]_0 (F_{C_4AF} - F_{C_4AF}(t^*))\Delta\bar{V}_{C_4AF},\ t \geq t^* \qquad (18b)$$

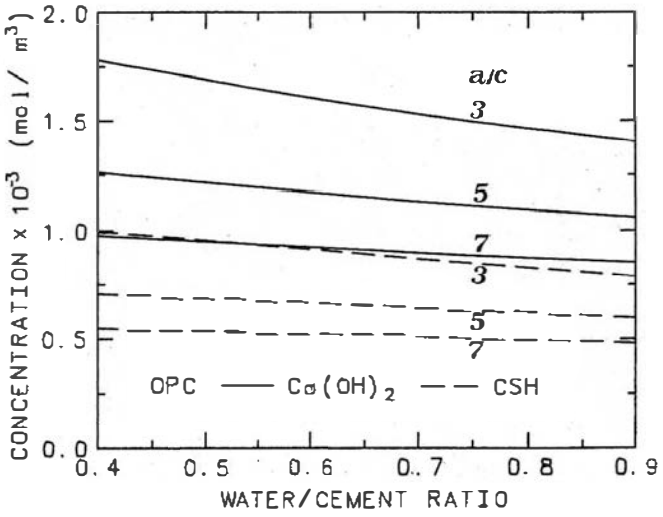


*Fig. 3—Effect of water-cement and aggregate-cement ratio on the molar concentration of carbonatable materials for completely hydrated OPC*

The term $\Delta\epsilon_c$ is due to the fact that the molar volumes of the solid products of the carbonation of $Ca(OH)_2$ and CSH exceed that of the molar volume of the materials reacting with $CO_2$, by $\Delta\bar{V}_{CH} = 3.85 \cdot 10^{-6}$ $m^3$/mol and $\Delta\bar{V}_{CSH} = 15.39 \cdot 10^{-6} m^3$/mol, respectively. Carbonation usually proceeds in the volume of concrete in the form of a front, separating a completely carbonated region from the rest, in which carbonation has not started yet.[27] In this latter region, the value of $\Delta\epsilon_c$ is zero, whereas in the former, $\Delta\epsilon_c$ is approximately equal to

$$\Delta\epsilon_c = [Ca(OH)_2]\,\Delta\bar{V}_{CH} + [CSH]\Delta\bar{V}_{CSH} \qquad (19)$$

in which the concentrations of $Ca(OH)_2$ and CSH are those at the completion of hydration.

Fig. 4 presents the porosity $\epsilon_p(t)$ of the hardened cement paste, which is related to the total porosity $\epsilon(t)$, as follows

$$\epsilon_p(t) = \epsilon(t)\left(1 + \frac{\frac{a}{c}\frac{\rho_c}{\rho_a}}{1 + \frac{w}{c}\frac{\rho_c}{\rho_w}}\right) \qquad (20)$$

The dependence of $\epsilon_p(t)$ on $w/c$ is shown separately for noncarbonated and carbonated concrete (or paste), the former for $t = 1$, 10, 100, and 1000 days, and the latter for $t = 100$ and 1000 days only. All the quantities in Fig. 4 (i.e., $\epsilon_0$, $\Delta\epsilon_H(t)$, $\Delta\epsilon_c$, and $\epsilon_p$) refer to unit volume of cement paste (plus entrapped or entrained air). Measured values of porosity are also shown in Fig. 4 for comparison. The experimental values were obtained gravimetrically, by comparison of the weights of fully water-saturated samples and oven-dried (at 105 C up to stabilization) ones.[13]

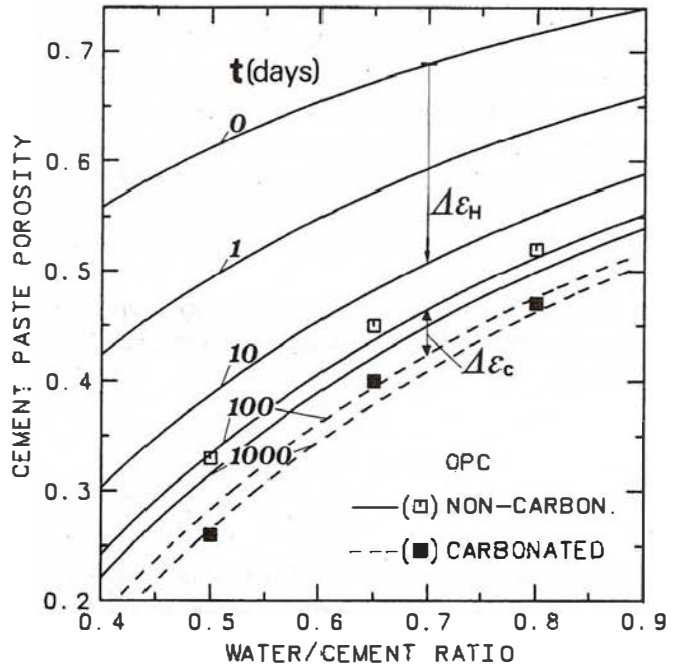


*Fig. 4—Dependence of cement paste porosity on age and water-cement ratio and comparison with measurements at* t = *100 days*

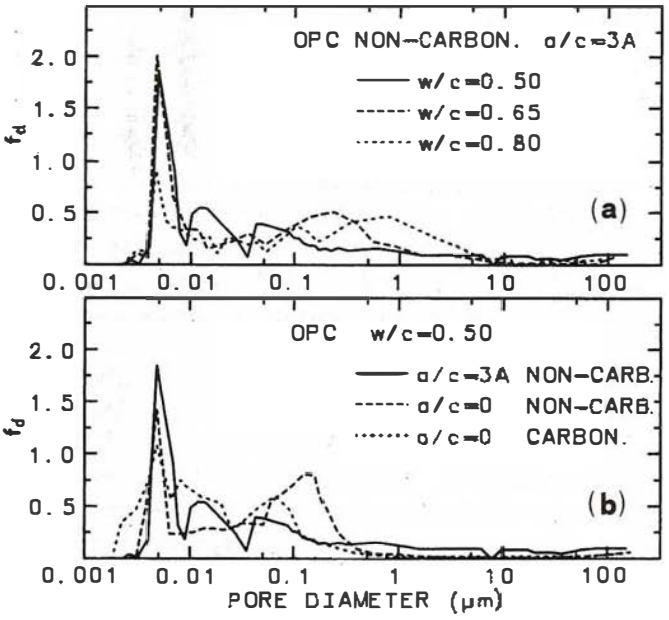


*Fig. 5—Pore-size distribution in fully hydrated hardened cement paste or mortar; (a) Effect of* w/c*; (b) Effect of carbonation and aggregates*

## PORE-SIZE DISTRIBUTION AND SPECIFIC SURFACE AREA OF PORES

The pore-size distribution (PSD) of concrete or hardened cement paste affects its effective diffusivity and controls the degree of saturation of the pores (for given relative humidity) and their specific surface area. Two methods mainly used today in research and by industry for the determination of the pore-size distribution of porous solids are: mercury porosimetry and nitrogen desorption according to the BET theory. Although some cement chemists[11-14] maintain that one of these methods is applicable to hardened cement paste

**Table 2—Composition and physical properties of portland cement—Gradation and physical properties of aggregates**

| Chemical composition of clinker; percent by weight | | | | | | |
|---|---|---|---|---|---|---|
| CaO | $SiO_2$ | $Al_2O_3$ | $Fe_2O_3$ | MgO | $SO_3$ | Residue |
| 65.28 | 23.55 | 6.12 | 2.51 | 1.30 | 0.47 | 0.77 |
| OPC: 94.9 percent clinker, 5.1 percent gypsum | | | | | | |
| Specific gravity: 3.16; fineness, according to Blaine test, 300 $m^2/kg$ | | | | | | |

| Aggregate gradation, percent by weight | | | | | | | | |
|---|---|---|---|---|---|---|---|---|
| Particle size | 1-½ in. | ½-⅜ in. | ⅜ in.-4 | 4-8 | 8-16 | 16-30 | 30-50 | 50- |
| Aggregate A | — | — | — | — | 20.5 | 40.4 | 19.0 | 20.1 |
| Aggregate B | 28.5 | 7.5 | 18.0 | 13.0 | 10.5 | 7.5 | 6.0 | 9.0 |
| Specific gravity: 2.61 | | | | | | | | |

for the entire spectrum of pore sizes, it is generally accepted today that for hardened cement paste, mercury porosimetry is not reliable for diameters below 60 to 100 Å, whereas nitrogen desorption is applicable for pore diameters only up to 300 to 500 Å. Moreover, the total surface area and the total pore volume of hardened cement paste, measured by either mercury porosimetry or nitrogen desorption, are lower than the ones measured gravimetrically on dried samples for pore volume or by X-ray scattering for surface area.[10,19] This result, which has been verified by the porosimetry measurements of the present study, has been interpreted as a strong indication that the pores of hardened cement paste with size below 10 to 15 Å are not accessible, not only to mercury but to nitrogen as well. This is not very surprising, since a similar behavior has been reported in the literature for coal, where pores below 10 to 15 Å have been found to be accessible to $CO_2$ but not to nitrogen.

The PSD of concrete has been determined herein by a combination of nitrogen desorption for small pore diameters with mercury porosimetry for large ones. The measurements from these two techniques were combined so that the same PSD was obtained on the average over their common range of application, i.e., between ~60 and ~500 Å.

Some measured pore-size distributions are presented herein in the form of the probability density function $f_d$ of the volume of pores with diameter equal to $d$ (in μm), which is defined so that the fraction of the total porosity of concrete, due to pores with the logarithm of $d$ ranging from log$d$ to log$d$ + $d$(log$d$), is equal to $f_d$ (log$d$) · $d$(log$d$). Pore-size distributions shown in Fig. 5 refer to essentially fully hydrated cement. The chemical composition and physical properties of cement are presented in Table 2. The aggregate used was a graded sand of Type A gradation (given in Table 2). Fig. 5(a) describes the effect of the water-cement ratio on the PSD of noncarbonated OPC mortar, with an aggregate-cement ratio equal to 3, whereas Fig. 5(b) shows the effect of carbonation on the PSD of hardened OPC paste with a water-cement ratio equal to 0.50. As is well known from previous studies,[11,14,18] the effect of reduc-

ing the $w/c$ is to shift the PSD to the left. As shown in Fig. 5(a), the shifting refers only to the macropores. On the contrary, the effect of carbonation is to shift the PSD to the left, over the entire range of pore diameters. Fig. 5(b) shows also the effect of the presence of aggregates.

The carbonation reactions (and other chemical reactions related to durability) take place at the interface of the pores and the solid volume of concrete, at a rate which is proportional to the specific surface area of the pores $a_s$, i.e., the total pore surface area per unit volume of concrete. The value of $a_s$ can be computed from the PSD and the porosity of concrete, or alternatively from the total pore surface area per unit weight of concrete $S$ (measured by water vapor or by the nitrogen adsorption method), the density of the solid phase $\varphi_s$, and the porosity of concrete, as follows

$$a_s = \epsilon \int_{-\infty}^{\infty} \frac{4}{d} f_d \, d(\log d) \tag{21a}$$

$$a_s = S\varphi_s (1 - \epsilon) \tag{21b}$$

## DEGREE OF SATURATION OF PORES

The degree of saturation of the pores with water $f$ is the fraction of the pore volume filled with water. Knowledge of $f$ is important for durability, because the fraction of the pore volume available for diffusion of gases, such as $CO_2$ for carbonation and $O_2$ for corrosion, equals $1 - f$, whereas it is in the remaining fraction of the pore volume, i.e., in $f$, that the diffusion of ions that dissolve the passivating layer of reinforcing bars, such as $Cl^-$, as well as the carbonation reaction of $Ca(OH)_2$ and $CO_2$ (with both of them dissolved in water), take place.

The degree of saturation can be computed if the PSD and the solid surface chemistry are known, assuming hygrothermal equilibrium between the pores and the environment. Under this condition, all pores with diameter less than the Kelvin diameter $d_K$ are completely filled with water, while the walls of all pores with diameters $d$ exceeding $d_K$ will be covered by a continuous film of water, of thickness $w$.[8,28,29] The values of $w$ and $d_K$ can be determined if the absolute temperature $T$ (K) and the relative humidity $RH$ (percent) are known (both in $\mu$m)

$$w = \frac{Cxd_w}{[1 + (C - 1)x](1 - x)} (1 - x^{d/2d_w}) \tag{22}$$

$$d_k = 2w + \frac{A}{T \ln (1/x)} \tag{23}$$

in which $x = RH/100$, the constant $A$ is equal to 0.6323 for noncarbonated material and to 0.2968 for carbonated, $C$ is the BET-constant for the particular temperature and water vapor-solid surface system, and $d_w$ is the molecular diameter of water (equal to $3 \cdot 10^{-4}$ $\mu$m). $C$-values for water vapor adsorption on some solid surfaces are given elsewhere.[8,21,29] From the present work it was found that for noncarbonated cements $C$ is approximately equal to 100 and for carbonated cements $C$ equals 1. This large difference in the values of $C$ and $A$ is due to the fact that the pore surface of noncarbonated concrete is hydrophilic, due to the presence of $Ca(OH)_2$, whereas that of carbonated concrete is not, due to its absence.

The completely filled pores, i.e., those with diameter $d < d_K$, take up the following fraction of the total pore volume

$$f_K = \int_{-\infty}^{\log d_K} f_d \, d(\log d) \tag{24}$$

whereas the aqueous film of the pores with diameter $d > d_K$ occupies the following fraction of the total volume of the pores

$$f_w = \frac{2\,Cxd_w}{[1 + (C-1)x](1-x)} \int_{\log d_K}^{\infty} \frac{1}{d} (1 - x^{d/2d_w}) f_d \, d(\log d) \tag{25}$$

The degree of saturation is the sum of $f_K$ and $f_w$

$$f = f_K + f_w \tag{26}$$

Fig. 6 shows experimentally observed values of $f$ as a function of the ambient $RH$ for several values of $w/c$, $a/c$, and fully carbonated or not cement by using the static method.[21] According to this method, the degree of saturation is computed from the steady-state weight of a concrete sample of known total volume, maintained in an environment of controlled relative humidity. Open symbols in Fig. 6 refer to data obtained by desorption (i.e., for reduction of relative humidity from 100 percent to 0), whereas filled ones refer to data obtained by adsorption of water. For the same value of $RH$, the value of $f$ obtained during desorption exceeds that obtained by adsorption. This hysteresis phenomenon is typical of drying processes in porous solids, and can be explained either by the extremely slow rate at which ultimate hygrothermal equilibrium is established (which implies that the actual state of equilibrium is in between those obtained by adsorption or desorption), or by the ink-bottle shape of the pores, resulting in water being trapped in the chambers along the pore during desorption or blocked from entering the chambers during adsorption.[21,29]

Fig. 6 also shows the results of the analytical relations Eq. (22) through (26), using in the latter the experimentally measured pore-size distributions. These "theoretical" values of $f$ lie close to the adsorption data for low relative humidities and the desorption ones for high, and are in between for intermediate relative humidities. This type of behavior is consistent with an ink-bottle shape of the pores.

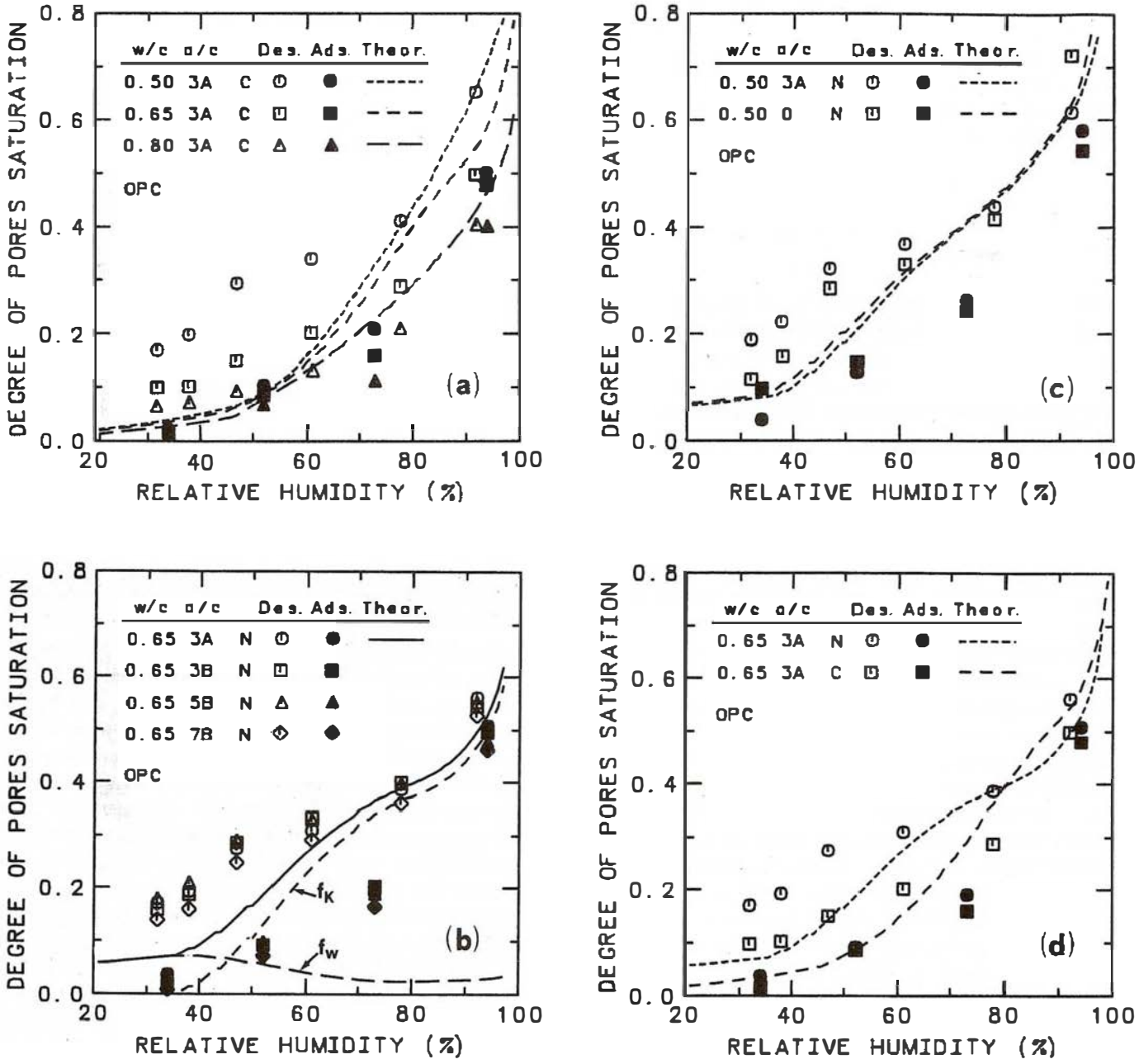


*Fig. 6—Effect of relative humidity on degree of saturation of the pores: (a) effect of* w/c*; (b) effect of* a/c *and aggregates gradation; (c) effect of aggregates' presence; (d) effect of carbonation (*C = *carbonated,* N = *noncarbonated)*

The dependence of $f$ on the water-cement ratio is shown in Fig. 6(a). For the same value of $RH$, $f$ decreases as the water-cement ratio increases, due to the reduction of the proportion of small-diameter pores in the PSD. Fig 6(b) and (c) show that the aggregate-cement ratio and the aggregate gradation have a negligible effect on $f$ (as shown in Table 2, aggregate A was a graded sand, and Aggregate B a mixture of sand and gravel). This is due to the fact that the presence and gradation of aggregates affect very little the proportion and the sizes of small-diameter pores. No theoretically obtained values of $f$ are shown in Fig. 6(b) for aggregate-cement ratios greater than 3.0 because, for such ratios, reliable measurements of the PSD by mercury porosimetry and by the BET technique were difficult to obtain. In the same figure, the contributions of $f_K$ and $f_w$ to the total value of $f$ are separated. Finally, Fig. 6(d) shows that, although carbonation increases the relative proportion of small-diameter pores, it causes a reduction in the value of $f$. This reduction is due to the chemistry of the pore surface, which corresponds to lower values of $A$ and $C$ in Eq. (23) and (25) and, hence, to less water in the pores of concrete after carbonation.

## EFFECTIVE GAS DIFFUSIVITY OF CONCRETE

The molecules of a gas $A$, such as $CO_2$, $O_2$ or water vapor, move within a medium such as air from regions

where the concentration (and hence the partial pressure) of gas $A$ is high to those where it is low. This transport mechanism of gases, called diffusion, follows Fick's first law

$$N_A = -D_A \frac{d[A]}{dx} \qquad (27)$$

in which $N_A$ is the rate of transfer of gas $A$ (in moles of $A$ per sec, per m² of the medium normal to the direction of the flux), $d[A]/dx$ is the concentration gradient of $A$ (in moles of $A$ per m, per m³ of the medium), and $D_A$ is the diffusion coefficient or diffusivity of $A$ within the medium in question (in m²/sec). In porous media, like concrete, diffusion of gases essentially takes place only within the gaseous phase of the pores. Nevertheless, it is more convenient to use in Eq. (27) "effective" values of $N_A$ and $D_A$, which refer to the total cross-sectional area of the porous medium normal to the direction of the flux and not just to that of the gaseous phase of the pores. The subscript $e$ is used to denote these effective values, so the effective diffusivity of gas $A$ is denoted by $D_{e,A}$.

Diffusivity should not be confused with permeability, which is the coeficient $K_A$ in Darcy's law considered to govern the convective flow of a fluid (gas or liquid) $A$ through a porous medium, due to a gradient in total pressure $dP/dx$ and not in partial pressure, the latter being proportional to $d[A]/dx$ in Eq. (27). With the exception of concrete structures containing liquids or gases under pressure, total pressure gradients are very uncommon in concrete structures, so the flow of gases or water through the pores of concrete is not the most important transport mechanism for the substances affecting durability (capillary flow due to capillary suction, which may serve as a transport mechanism for ions or others substances, is not considered herein, as it is a transient phenomenon, contributing to the establishment of the hygrothermal equilibrium in the pores assumed in this work). The dominant transport mechanism is diffusion of molecules or ions in the gaseous or aqueous phase of the pores, according to Eq. (27).

From the point of view of durability of reinforced concrete, we are interested in the diffusion of $CO_2$ and $O_2$ through the gas phase of the pores, as it is the former that carbonates the $Ca(OH)_2$ of the hardened cement paste, therefore reducing the alkalinity of concrete, and it is the latter that oxidizes the already depassivated (because of the drop in alkalinity or chloride penetration or both) reinforcing bars. The effective diffusivity of a gas $A$, $D_{e,A}$ is inversely proportional to the square root of its molar weight $MW_A$ since, in concrete Knudsen diffusion controls,[30] as the mean free path $\lambda$ of gases is of the same order as the pore diameter. So, the effective diffusivity of a gas $B$, $D_{e,B}$ can be obtained from that of $A$ by multiplying it by $(MW_A/MW_B)^{1/2}$. This concept can be applied to find the effective diffusivity of $CO_2$, $D_{e,CO_2}$ from that of $N_2$, which is easier to measure experimentally, as $N_2$ is inert with respect to concrete, by multiplying the latter by 0.80. Similarly, the effective diffusivity of $O_2$ can be computed from that of $CO_2$ by multiplying it by 1.17.

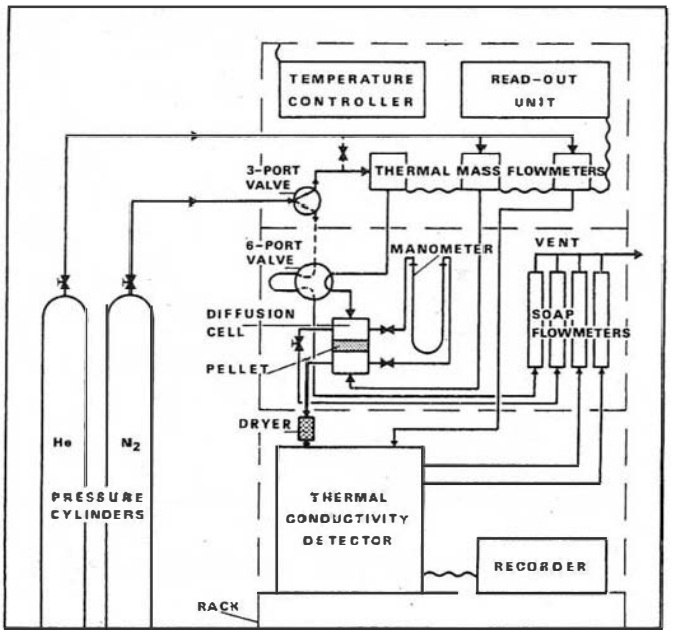


*Fig. 7—Schematic diagram of the effective diffusivity measurement apparatus (steady-state operation; dashed lines: dynamic operation)*

The effective diffusivity of a gas in a porous medium can be found theoretically or experimentally.[30] Most of the theoretical models[31-36] require a geometrical model of the pore system (such as the parallel pore model[31] or the random pore model[32]) and knowledge of some measurable physical properties of the medium, such as mass density of the solid phase, porosity, pore-size distribution, and specific surface area of the pores, to convert the diffusivity of gas $A$ in the gaseous phase of the pores to effective diffusivity of the porous medium. Effective diffusivity can also be determined experimentally[30,37-39] using a setup originally proposed by Wicke and Kallenbach. Such a setup was constructed in our laboratory, as shown in Fig. 7 and 8, to measure the effective diffusivity in mortar and hardened cement paste.

The mortar or paste specimens used were in the form of cylindrical pellets, with 25.5 mm diameter and 10 mm height. The pellets were cast within a polyvinyl chloride PVC ring-like mold, the interior surface of which was covered prior to casting with an epoxy resin to achieve leak-tightness of the concrete-mold interface. Specimens were cured for 3 months in 30 C water to achieve complete hydration. Then the specimens were placed for several days in a chamber of constant and controlled relative humidity to achieve a steady-state degree of saturation in the pores. Before trasfering them from this chamber to the diffusion cell for testing, the specimens were weighed accurately to develop a unit weight-versus-relative humidity curve for the specific composition of the specimen. Afterwards, the specimens with the PVC ring around them were placed in the diffusion cell of the apparatus, as shown in Fig. 8.

As shown in Fig. 7 and 8, $N_2$ and He gases flow through the upper and lower chamber of the cell, respectively. The flow rates are held constant during the test by means of thermal mass flowmeter controllers. To eliminate convective transport through the pellet, the pressure is maintained the same in both chambers by means of a needle valve in the upper chamber outlet and a manometer interposed between the two chambers. After steady-state is achieved, the molar fraction $y_{N_2}$ of $N_2$ in the helium stream is measured by means of a thermal conductivity detector. Then the effective diffusivity of the $N_2$ that diffuses from the upper stream to the lower can be computed from the relation

$$D_{e,N_2} = \frac{F_l y_{N_2}}{(1 - y_{N_2})} \frac{1}{s} \tag{28}$$

in which $F_l$ is the flow rate of helium through the lower chamber ($m^3$/sec), $s$ is the cross-sectional area of the pellet ($m^2$), and $l$ is its length (m). After removal from the cell, the specimen was weighed again, and its weight was compared to that before testing, to detect any change in its water content. If such a change was found, the unit weight-versus-relative humidity curve developed from the weighing operation prior to testing for this particular specimen composition was used to determine the ambient relative humidity corresponding to the average degree of saturation of the specimen during testing.

Effective $CO_2$ diffusivity values, computed from the ones measured for $N_2$, are shown as data points in Fig. 9 as a function of relative humidity and concrete composition parameters. Fig. 9(a) shows that an increase in the value of water-cement ratio increases drastically the value of diffusivity, as it increases porosity and the mean pore diameter. Fig. 9(b) presents the effect of the absence of aggregates (open circles) and carbonation (open squares) on the value of the diffusivity coefficient. The data presented, as well as experimental results by others,[17,25] show that there is essentially no difference in diffusivity between concrete (filled circles)

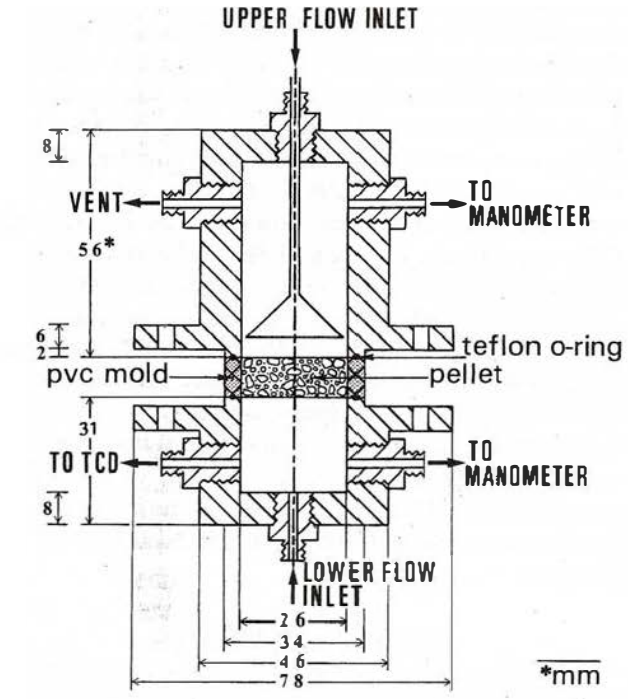


*Fig. 8—Diffusion cell*

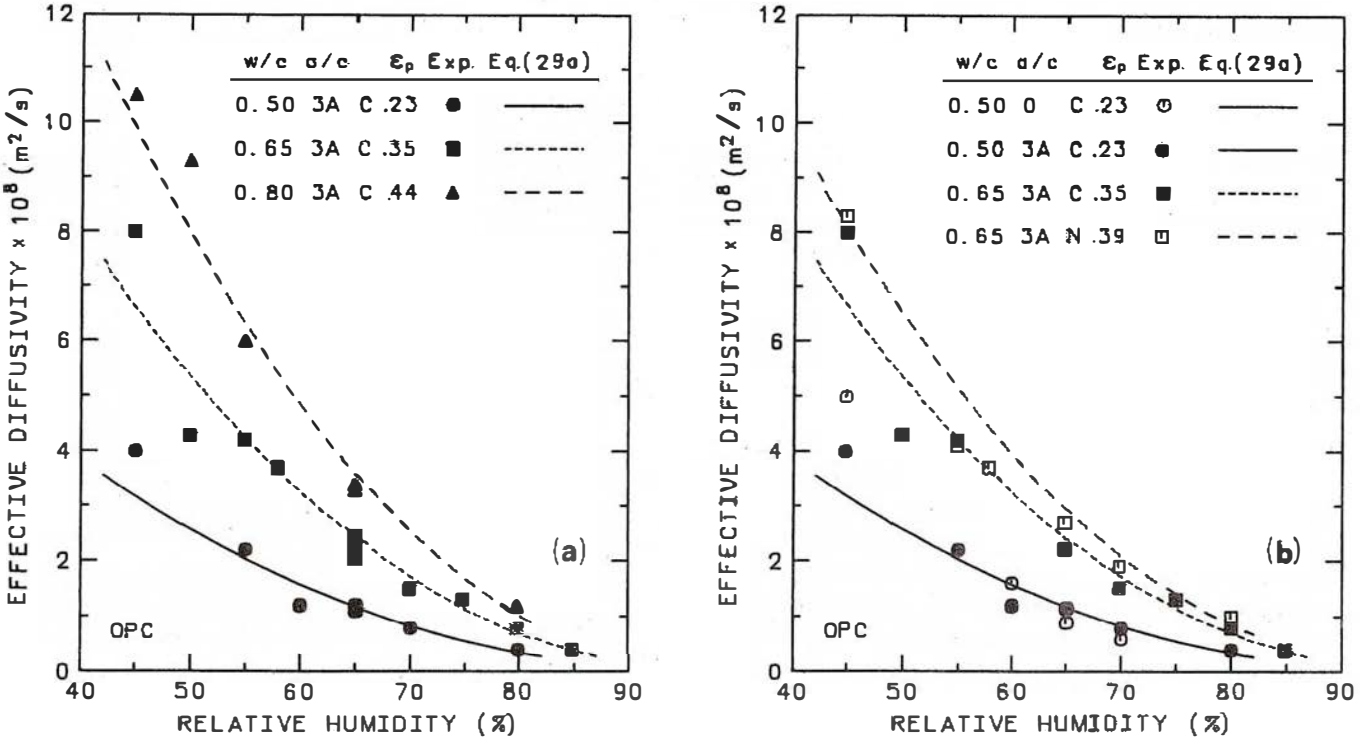


*Fig. 9—Dependence of effective diffusivity of $CO_2$ in concrete on relative humidity, water-cement ratio, presence of aggregates and carbonation (C = carbonated, N = noncarbonated)*

and cement paste (open circles) specimens, as long as the water-cement ratio and the type of cement are the same. In other words, the presence of aggregates does not seem to affect significantly the value of effective diffusivity, apparently because diffusion along the aggregate-paste interface makes up for the lack of diffusion through the aggregate particles themselves. Therefore, the value of effective diffusivity is considered herein as a function of the porosity of hardened cement paste $\epsilon_p(t)$, given by Eq. (20). Carbonation is found to reduce diffusivity, as it reduces the value of $\epsilon_p$. The significant effect of relative humidty can be taken into account by considereing the value of $D_e$ as a function of $f$, which also includes the effect of pore-size distribution. Alternatively, the effective diffusivity can be considered directly as a function of $(1 - RH/100)$.

Regression analysis of the experimental data yielded the following expression for the effective diffusivity of $CO_2$ (in $m^2$/sec)

$$D_{e,CO_2} \approx 1.64 \cdot 10^{-6} \epsilon_p^{1.8} (1 - RH/100)^{2.2} \quad (29a)$$

The predictions of Eq. (29a) are also presented in Fig. 9, and are in good agreement with the corresponding experimental data. The effective diffusivity of $O_2$ is given by

$$D_{e,O_2} = 1.92 \cdot 10^{-6} \epsilon_p^{1.8} (1 - RH/100)^{2.2} \quad (29b)$$

It is worth mentioning that the latest draft of the CEB 1990 Model Code[40] states in Chapter 2.1.9 ("Transport of Liquids and Gases in Hardened Concrete") that the effective diffusivity of $CO_2$ and $O_2$ in concrete is in the range $0.5 \cdot 10^{-8}$ to $6 \cdot 10^{-8}$ $m^2$/sec, and proposes the following expression for concrete "sheltered from rain" (meaning relative humidity around 60 percent)

$$D_{e,CO_2} \text{ (m}^2\text{/sec)} = 10^{-7} \cdot 10^{-0.025 f_{ck}} \quad (30)$$

in which $f_{ck}$ is the characteristic compressive strength of the concrete in MPa. For concrete exposed to rain (meaning relative humidity around 70 percent, it is proposed to reduce the values given by Eq. (30) by 50 percent. Eq. (29a) is in good overall agreement with these code proposals, but gives a more complete quantitative description of the dependence of the effective diffusivity on the controlling variables.

## CONCLUSIONS AND SUMMARY

In this paper, quantitative information is given on some physical and chemical characteristics of concrete on which its durability depends. This information can be used as input data to quantitative models of the processes that lead to deterioration of concrete and reinforced concrete, such as carbonation.[27]* Specifically, the evolution in time of the concentration of carbonatable constituents of hardened and noncarbonated cement paste, $Ca(OH)_2$, CSH, $C_3S_1$ and $C_2S$, are given by Eq. (10) through (13) in terms of their initial concentrations given by Eq. (14) and (16) and the evolution of hydration described by Eq. (8) and Table 1. The evolution of the porosity of concrete with time, as affected by the evolution of hydration and the occurrence of carbonation, is also computed analytically [Eq. (16) through (19)]. Pore-size distributions as measured by a combination of two techniques, so that the entire spectrum of the distribution can be obtained, are presented as functions of the composition of concrete, etc. (Fig. 5). From the computed porosity and the measured pore-size distributions, the specific surface area of the pores can be obtained from Eq. (21). The maximum diameter of concrete pores that are completely filled with water, and the thickness of the aqueous film covering the walls of the rest, are given by Eq. (22) and (23), respectively, in terms of the ambient relative humidity. The volume of water in these two groups of pores are computed by Eq. (24) and (25), giving the degree of saturation of the pores [Eq. (26)]. Finally, the effective diffusivity of gases in concrete, such as $CO_2$ or $O_2$, is measured for various compositions of concrete and values of the ambient relative humidity. Empirical expressions, Eq. (29a) and (29b), fitted to the test results, give the effective diffusivity in terms of the porosity of the paste and the relative humidity of the ambient air.

*Papadakis, V. G.; Vayenas, C. G.; and Fardis, M. N., "Fundamental Modeling and Experimental Investigation of Concrete Carbonation," submitted to the *ACI Materials Journal*, 1989.

## ACKNOWLEDGMENTS

The Hellenic General Secretariat for Research and Technology, and the Institute of Chemical Engineering and High Temperature Chemical Processes have provided financial support for this work. Thanks are also due to Dr. E. Galanoulis of the TITAN Inc. cement company for helpful discussions and technical support provided.

## REFERENCES

1. Comite Euro-International du Beton, "Durability of Concrete Structures: State-of-the-Art Report," *Bulletin d'Information*, No. 148, Paris, 1982, 328 pp.

2. Comite Euro-International du Beton, "Durable Concrete Structures: CEB Design Guide," *Bulletin d'Information*, No. 182, Lausanne, 1989, 268 pp.

3. Brunauer, S., and Copeland, L. E., "Chemistry of Concrete," *Scientific American*, V. 210, No. 4, 1964, pp. 80-92.

4. Lea, F. M., *Chemistry of Cement and Concrete*, 3rd ed., Edward Arnold Ltd., London, 1970, pp. 114, 177-310.

5. Bensted, J., "Hydration of Portland Cement," *Advances in Cement Technology*, S. N. Ghosh, ed., Pergamon Press, New York, 1983, pp. 307-347.

6. Frigione, G., "Gypsum in Cement," *Advances in Cement Technology*, S. N. Ghosh, ed., Pergamon Press, New York, 1983, pp. 485-535.

7. Taylor, H. F. W., "Chemistry of Cement Hydration," *Proceedings*, 8th International Congress on the Chemistry of Cement, Rio de Janeiro, 1986, V. I, pp. 82-110.

8. Hagymassy, J. Jr.; Brunauer, S.; and Mikhail, R. Sh., "Pore Structure Analysis by Water Vapor Adsorption I. T-Curves for Water Vapor," *Journal of Colloid and Interface Science*, V. 29, No. 3, 1969, pp. 485-492.

9. Bodor, E. E.; Skalny, J.; Brunauer, S.; Hagymassy, J. Jr.; and Yudenfreund, M., "Pore Structures of Hydrated Calcium Silicates and Portland Cements by Nitrogen Adsorption," *Journal of Colloid and Interface Science*, V. 34, No. 4, 1970, pp. 560-570.

10. Mikhail, Raouf Sh.; Turk, Danica H.; and Brunauer, Stephen, "Dimensions of the Average Pore, the Number of Pores, and the Surface Area of Hardened Portland Cement Paste," *Cement and Concrete Research*, V. 5, No. 5, 1975, pp. 433-442.

11. Manmohan, D., and Mehta, P. K., "Influence of Pozzolanic Slag, and Chemical Admixtures on Pore Size Distribution and Permeability of Hardened Cement Pastes," *Cement, Concrete and Aggregates*, V. 3, No. 1, 1981, pp. 63-67.

12. Feldman, R. F., "Significance of Porosity Measurements on Blended Cement Performance," *Fly Ash, Silica Fume, Slag and Other Mineral By-Products in Concrete—Proceedings, 1st International Conference*, SP-79, V. 1, American Concrete Institute, Detroit, 1983, pp. 415-433.

13. Hansen, Torben C., "Physical Structure of Hardened Cement Paste. A Classical Approach," *Materials and Structures, Research and Testing* (RILEM, Paris), V. 19, No. 114, pp. 423-436.

14. Odler, I., and Koster, H., "Investigations on the Structure of Fully Hydrated Portland Cement and Tricalcium Silicate Pastes. II. Total Porosity and Pore Size Distribution," *Cement and Concrete Research*, V. 16, No. 6, Nov. 1986, pp. 893-901.

15. Litvan, G. G., and Meyer, A., "Carbonation of Granulated Blast Furnace Slag Cement Concrete During Twenty Years of Field Exposure," *Fly Ash, Silica Fume, Slag and Natural Pozzolans in Concrete—Proceedings, 2nd International Conference*, SP-91, V. 2, American Concrete Institute, Detroit, 1986, pp. 1445-1462.

16. Gunter, M.; Bier, Th.; and Hilsdorf, H., "Effect of Curing and Type of Cement on the Resistance of Concrete to Freezing in Deicing Salt Solutions," *Concrete Durability—Katharine and Bryant Mather International Conference*, SP-100, V. 1, American Concrete Institute, Detroit, 1987, pp. 877-899.

17. Schiessl, P., "Influence of the Composition of Concrete on the Corrosion Protection of the Reinforcement," *Concrete Durability—Katharine and Bryant Mather International Conference*, SP-100, V. 2, American Concrete Institute, Detroit, 1987, pp. 1633-1650.

18. Ying-yu, L., and Qui-dong, W., "Mechanism of Carbonation of Mortar and the Dependence of Carbonation on Pore Structure," *Concrete Durability—Katharine and Bryant Mather International Conference*, SP-100, V. 2, American Concrete Institute, 1987, pp. 1915-1943.

19. Day, Robert L., and Marsh, Bryan K., "Measurement of Porosity in Blended Cement Pastes," *Cement and Concrete Research*, V. 18, No. 1, Jan. 1988, pp. 63-73.

20. Young, J. F., "Review of Pore Structure of Cement Paste and Concrete and Its Influence on Permeability," *Permeability of Concrete*, SP-108, American Concrete Institute, Detroit, 1988, pp. 1-8.

21. Keey, R. B., *Drying, Principles and Practice*, Pergamon Press, Oxford, 1972, pp. 19-49.

22. Bazant, Z. P., and Najjar, L. J., "Drying of Concrete as a Nonlinear Diffusion Problem," *Cement and Concrete Research*, V. 1, No. 5, 1971, pp. 461-473.

23. Lawrence, C. D., "Transport of Oxygen through Concrete," *Proceedings*, British Ceramic Society Meeting on Chemistry and Chemically-Related Properties of Cement, London, 1984, pp. 277-293.

24. Tuutti, Kyosti, "Corrosion of Steel in Concrete," *CBI Forskning Research*, Swedish Cement and Concrete Research Institute, Stockholm, 1982, pp. 24-57.

25. Hurling, H., "Oxygen Permeability of Concrete," *Proceedings*, RILEM Seminar on the Durability of Concrete Structures under Normal Outdoor Exposure, RILEM, Hannover, 1984, pp. 91-101.

26. ACI Committee 211, "Recommended Practice for Selecting Proportions for Normal and Heavyweight Concrete (ACI 211.1-77)," *Manual of Concrete Practice*, Part 1, American Concrete Institute, Detroit, 1979, 20 pp.

27. Papadakis, V. G.; Vayenas, C. G.; and Fardis, M. N., "Reaction Engineering Approach to the Problem of Concrete Carbonation," *Journal of the American Institute of Chemical Engineers (AIChE Journal)*, V. 35, No. 10, 1989, pp. 1639-1650.

28. Gregg, S. J., and Sing, K. S. W., *Adsorption, Surface Area and Porosity*, 2nd ed., Academic Press, London, 1982, pp. 248-282.

29. Mikhail, R. Sh., *Microstructure and Thermal Analysis of Solid Surfaces*, John Wiley & Sons, New York, 1983, pp. 22-72.

30. Smith, J. M., *Chemical Engineering Kinetics*, 3rd ed., McGraw-Hill, New York, 1981, pp. 450-473.

31. Wheeler, A., in Emmett, P. H., ed., *Catalysis*, V. II, Ch. 2, Reinhold Publishing Corporation, New York, 1955, p. 105.

32. Wakao, N., and Smith, J. M., "Diffusion in Catalyst Pellets," *Chemical Engineering Science*, V. 17, 1962, pp. 825-834.

33. Johnson, M. F. L., and Stewart, W. E., "Pore Structure and Gaseous Diffusion in Solid Catalysts," *Journal of Catalysis*, V. 4, 1965, pp. 248-252.

34. Feng, C., and Stewart, W. E., "Practical Models for Isothermal Diffusion and Flow of Gases in Porous Solids," *Industrial and Engineering Chemistry Fundamentals*, V. 12, No. 2, 1973, pp. 143-147.

35. Carniglia, S. C., "Construction of Tortuosity Factor from Porosimetry," *Journal of Catalysis*, V. 102, 1986, pp. 401-418.

36. Burganos, V. N., and Sotirchos, S. V., "Diffusion in Pore Networks: Effective Medium Theory and Smooth Field Approximation," *Journal of the American Institute of Chemical Engineers (AIChE Journal)*, V. 33, No. 10, 1987, pp. 1678-1689.

37. Dogu, G., and Smith, J. M., "Dynamic Method for Catalyst Diffusivities," *Journal of the American Institute of Chemical Engineers (AIChE Journal)*, V. 21, No. 1, 1975, pp. 58-61.

38. Burghardt, A., and Smith, J. M., "Dynamic Response of a Single Catalyst Pellet," *Chemical Engineering Science*, V. 34, 1979, pp. 267-273.

39. Dogu, T.; Keskin, A.; Dogu, G.; and Smith, J. M., "Single-Pellet, Moment Method for Analysis of Gas-Solid Reactions," *Journal of the American Institute of Chemical Engineers (AIChE Journal)*, V. 32, No. 5, 1986, pp. 743-750.

40. Comite Euro-International du Beton, "CEB-FIP Model Code 1990," *Bulletin d'Information*, No. 195, 196, Lausanne, 1990.